nature chemical biology

ARTICLE

PUBLISHED ONLINE: 2 OCTOBER 2017 | DOI: 10.1038/NCHEMBIO.2486

Inhibition of USP10 induces degradation of oncogenic FLT3

Ellen L Weisberg[1,6]*, Nathan J Schauer[2,6], Jing Yang[2,6], Ilaria Lamberto[2,6], Laura Doherty[2], Shruti Bhatt[1], Atsushi Nonami[1], Chengcheng Meng[1], Anthony Letai[1], Renee Wright[1], Hong Tiv[3], Prafulla C Gokhale[3], Maria Stella Ritorto[4], Virginia De Cesare[4], Matthias Trost[4], Alexandra Christodoulou[1], Amanda Christie[1], David M Weinstock[1], Sophia Adamia[1], Richard Stone[1], Dharminder Chauhan[1], Kenneth C Anderson[1], Hyuk-Soo Seo[2], Sirano Dhe-Paganon[2], Martin Sattler[1], Nathanael S Gray[2,5], James D Griffin[1] & Sara J Buhrlage[2,5]*

Oncogenic forms of the kinase FLT3 are important therapeutic targets in acute myeloid leukemia (AML); however, clinical responses to small-molecule kinase inhibitors are short-lived as a result of the rapid emergence of resistance due to point mutations or compensatory increases in FLT3 expression. We sought to develop a complementary pharmacological approach whereby proteasome-mediated FLT3 degradation could be promoted by inhibitors of the deubiquitinating enzymes (DUBs) responsible for cleaving ubiquitin from FLT3. Because the relevant DUBs for FLT3 are not known, we assembled a focused library of most reported small-molecule DUB inhibitors and carried out a cellular phenotypic screen to identify compounds that could induce the degradation of oncogenic FLT3. Subsequent target deconvolution efforts allowed us to identify USP10 as the critical DUB required to stabilize FLT3. Targeting of USP10 showed efficacy in preclinical models of mutant-FLT3 AML, including cell lines, primary patient specimens and mouse models of oncogenic-FLT3-driven leukemia.

The ubiquitin system plays a critical role in controlling protein homeostasis, a process necessary for cell health. Ubiquitination is a reversible post-translational modification whose best-known and best-characterized function is the tagging of proteins for proteolytic degradation[1]. However, its importance in protein activation/inactivation, localization, and lysosomal and autophagic degradation, among other cellular processes, is becoming increasingly appreciated[2]. Ubiquitin is a 76-amino-acid protein that attaches to substrate proteins via isopeptide-bond formation between ubiquitin's C-terminal glycine and a substrate lysine side chain; linear and branched polyubiquitin chains are assembled via the attachment of a new ubiquitin molecule to one of seven lysines or the N-terminal methionine of ubiquitin[3]. Ubiquitination is coordinated by the action of ubiquitin-activating (E1), -conjugating (E2) or -ligating (E3) enzymes and by DUBs. DUBs have garnered considerable interest as drug targets in recent years because of their role in the stabilization of disease-causing proteins, and oncology targets in particular[4].

At present, there are approximately 115 recognized human DUBs belonging to six distinct families[5,6]. The substrates of DUBs, and the contexts in which they are regulated, remain poorly understood[7]. Most studies aimed at the identification of the DUB responsible for the stabilization of a substrate of interest use a genetic-based screen to measure protein levels or a mass-spectrometry-based approach to identify DUBs that interact with the target[7,8]. Chemical probes have been developed to allow the pharmacological interrogation of DUBs identified from such screens, and more than 40 DUB inhibitors are now reported[9].

The screening of annotated enzyme-family-specific small-molecule libraries has been used successfully—in the kinase family, for example[10,11]—as a complementary approach to discover disease targets. This middle-of-the-road approach between a completely target-unbiased small-molecule phenotypic screen, in which target deconvolution can be extraordinarily difficult, and inhibitor development focused on a single putative target that might not be ideal for pharmacological inhibition can be powerful for discovering new and druggable dependencies of a disease. This approach, to the best of our knowledge, has not been applied to DUBs, probably in large part because of the lack of well-characterized, commercially available DUB-targeting small-molecule libraries.

AML is the most common type of acute leukemia in adults. Approximately 30% of people with AML harbor activating mutations in *FLT3*, a gene that normally functions in the control of hematopoiesis. The most common type of *FLT3* mutation results in internal tandem duplications (ITDs) in the juxtamembrane domain, observed in 20–25% of AML patients and associated with markedly decreased survival[12]. An additional 7% of those with AML have point mutations within the 'activation loop' of *FLT3* (ref. 12).

Mutant FLT3 is a clinically validated target. A number of FLT3 kinase domain inhibitors have been shown to induce partial, and usually brief, remission when administered alone in clinical trials of relapsed AML patients[13]. In a large trial (RATIFY (CALGB-10603)) in newly diagnosed patients, however, midostaurin (PKC412) was shown to increase survival when administered in combination with standard chemotherapy[14]. This study in particular supports the notion that the inhibition of FLT3 is important, at least in subjects

[1]Department of Medical Oncology, Dana-Farber Cancer Institute, Harvard Medical School, Boston, Massachusetts, USA. [2]Department of Cancer Biology, Dana-Farber Cancer Institute, Harvard Medical School, Boston, Massachusetts, USA. [3]Experimental Therapeutic Core, Dana-Farber Cancer Institute, Harvard Medical School, Boston, Massachusetts, USA. [4]MRC Protein Phosphorylation and Ubiquitylation Unit, University of Dundee, Dundee, Scotland, UK. [5]Department of Biological Chemistry and Molecular Pharmacology, Harvard Medical School, Boston, Massachusetts, USA. [6]These authors contributed equally to this work *e-mail: ellen_weisberg@dfci.harvard.edu or saraj_buhrlage@dfci.harvard.edu

with mutations in *FLT3*. Because drug resistance develops in some patients with newly diagnosed AML and in virtually all patients with advanced disease, additional strategies for targeting FLT3 would be valuable.

As is true of other receptor tyrosine kinases, synthesis and degradation of FLT3 in the body are ongoing, and are thought to be accelerated by ligand binding. FLT3 turnover has been shown to be regulated via ubiquitin-mediated proteosomal and lysosomal degradation, and the ubiquitin ligase c-Cbl targets FLT3 for ubiquitination and degradation[15]. In addition, inactivating point mutations in c-Cbl have been found in myeloid malignancies[16], which underscores the importance of tight choreography of FLT3 turnover in disease progression.

Here we report the use of a focused DUB-inhibitor library screen to identify USP10 as the DUB that stabilizes the FLT3-ITD oncoprotein via the removal of a degradative ubiquitin tag. Furthermore, we show that pharmacological inhibition of USP10 promotes the degradation of FLT3-ITD but not of wild-type FLT3, leads to selective killing of oncogenic-FLT3-expressing AML cells *in vitro* and *in vivo*, and overrides resistance to FLT3 kinase inhibitors caused by tyrosine kinase domain (TKD) mutations and other mechanisms. Our results thus validate USP10 as a therapeutic target for FLT3-mutant AML. To the best of our knowledge, this is the first novel DUB substrate to be identified by a DUB-targeting small-molecule library screen, and the first demonstration of the stabilization of a mutant driver oncoprotein in AML by a DUB enzyme.

RESULTS

HBX19818 and P22077 induce degradation of mutant FLT3

To identify targets and compounds that regulate the protein homeostasis of oncogenic FLT3, we used a whole-cell phenotypic screen of 29 reported small-molecule DUB inhibitors (**Supplementary Results**, **Supplementary Table 1**), representing the majority of reported DUB inhibitors, annotated for inhibitory activity across a broad panel of DUBs (ref. 17 and data not shown) with oncogene-dependent and control cell lines, followed by hit validation, target deconvolution and translational studies (**Supplementary Fig. 1a**). We evaluated compounds for their ability to selectively kill growth-factor-independent Ba/F3 cells expressing FLT3-ITD mutant protein and Ba/F3 cells expressing FLT3-D835Y mutant protein versus IL-3-dependent parental Ba/F3 cells. Two chemically distinct hits from the screen, HBX19818 (**1**) and P22077 (**2**) (**Fig. 1a**), both previously reported as USP7 inhibitors[18,19], were confirmed to inhibit the proliferation of mutant-FLT3-positive Ba/F3 cells with values of effector concentration for a half-maximum response (EC_{50}) in the single-digit micromolar range (**Fig. 1b**,**c**, **Supplementary Fig. 1b**). The effects were partially rescued by IL-3, indicating that the growth suppression resulted from impaired FLT3 function. The antiproliferative activity of HBX19818 and P22077 correlated with the loss of FLT3 in FLT3-ITD-expressing Ba/F3 cells at the same concentrations, and with a more modest loss of FLT3 in FLT3-D835Y-expressing Ba/F3 cells (**Fig. 1d**,**e**, **Supplementary Fig. 1c**). Consistent with this, flow cytometry showed a loss of cell-surface expression of FLT3-ITD after treatment with HBX19818 (**Supplementary Fig. 1d**). In contrast, FLT3 levels were unchanged in inhibitor-treated Ba/F3 cells that expressed wild-type FLT3 (**Fig. 1f**, **Supplementary Fig. 1e**). Owing to a lack of FLT3-D835Y-positive cell lines, in our subsequent studies we focused on the FLT3-ITD mutant.

We confirmed that the effects of HBX19818 and P22077 on cells that expressed mutant FLT3 were not unique to the Ba/F3 system. Both compounds suppressed the growth of the FLT3-ITD-positive AML cell lines MOLM13-luc+, MOLM14 and MV4,11 in a dose-dependent manner with selectivity toward mutant-FLT3-expressing cells versus cells that expressed the wild-type protein or FLT3-null cells (**Fig. 2a**, **Supplementary Fig. 2a**, **Supplementary Table 2**). It should be noted, however, that several human hematopoietic cell lines not driven by oncogenic FLT3 showed relative sensitivity to P22077, which can probably be attributed to the multi-targeted nature of this agent. Treatment with HBX19818 and P22077 led to increased priming of mutant-FLT3-expressing cells for apoptosis that strongly correlated with the induction of apoptosis and that was stronger for cells expressing mutant FLT3 than for those expressing wild-type or no FLT3 (**Supplementary Fig. 2b–g**). Consistent with data for the Ba/F3 system, HBX19818 and P22077 strongly induced FLT3 degradation in the FLT3-ITD-positive lines MOLM13-luc+ and MOLM14 at 20 μM (**Fig. 2b**, **Supplementary Fig. 3a**,**b**) but

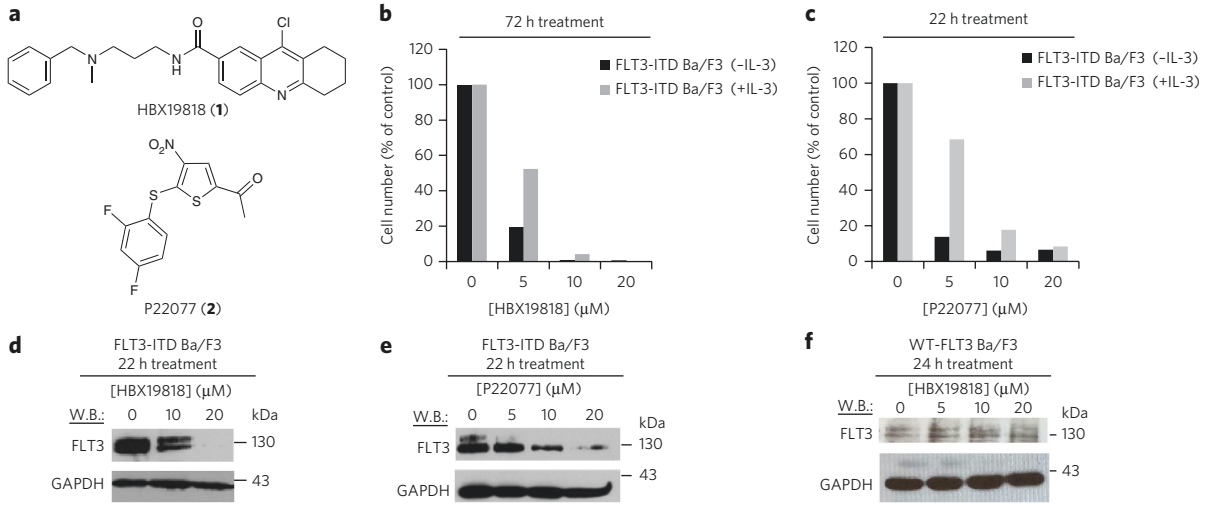

Figure 1 | Targeted effects of HBX19818 and P22077 on Ba/F3 cells expressing mutant or wild-type FLT3. (**a**) The chemical structures of HBX19818 (**1**) and P22077 (**2**). (**b**) The effects of HBX19818 on FLT3-ITD-expressing Ba/F3 cells cultured in the absence or presence of 20% WEHI-conditioned media (used as a source of IL-3) after 72 h of treatment ($n = 2$). (**c**) The effects of P22077 on FLT3-ITD-expressing Ba/F3 cells cultured in the absence or presence of 20% WEHI-conditioned media (used as a source of IL-3) after 22 h of treatment ($n = 2$). (**d**) The effects of HBX19818 on FLT3 expression in FLT3-ITD-expressing Ba/F3 cells after 22 h of treatment. (**e**) The effects of P22077 on FLT3 levels in FLT3-ITD-expressing Ba/F3 cells after 22 h of treatment. (**f**) The effects of HBX19818 on FLT3 protein levels in Ba/F3 cells expressing wild-type (WT) FLT3 after 24 h of treatment. The immunoblots shown are representative of 1–2 additional studies for which similar results were observed. W.B., western blotting.

had little to no effect on FLT3 levels in leukemia cell lines expressing wild-type FLT3 (**Supplementary Fig. 3c**,**d**). As anticipated, we observed inhibition of total cellular tyrosine phosphorylation in HBX19818-treated mutant-FLT3-positive cells, consistent with drug-induced degradation of mutant FLT3 (**Supplementary Fig. 3e**). Treatment with HBX19818 or P22077 did not lead to the degradation of signaling molecules downstream of FLT3, including AKT and ERK1/ERK2, which suggests that the compounds' induction of mutant-FLT3 degradation was selective (**Fig. 2b**).

Compounds induce ubiquitin-mediated degradation of FLT3

Consistent with the loss of FLT3 resulting from ubiquitin-dependent degradation, we observed increased FLT3 ubiquitination for FLT3-ITD 4–8 h after HBX19818 treatment (**Fig. 2c**). Ubiquitin tags can encode proteosomal or lysosomal degradation; FLT3 has been reported to undergo degradation by both pathways. We established that both HBX19818- and P22077-induced FLT3-ITD degradation were partially rescued by inhibition of the lysosome (**Fig. 2d**,**e**), and qPCR analysis confirmed that the reduction in FLT3 levels occurred at the protein level only (**Fig. 2f**).

Structure–activity relationship studies

HBX19818 and P22077 have both been reported as irreversible inhibitors of ubiquitin-specific protease 7 (USP7), a DUB best known for its role in the stabilization of MDM2 (refs. 18,19). Using diubiquitin as substrate[17], we profiled the compounds *in vitro* against a panel of 33 recombinant DUBs at a concentration of 10 μM and identified USP10 as the DUB most potently inhibited by each compound (**Supplementary Fig. 4a**,**b**). HBX19818 and P22077 inhibited USP10 with half-maximal inhibitory concentration (IC_{50}) values of 14 and 6 μM, respectively, and USP7 with IC_{50} values of 57 and 10 μM, respectively, when tested for dose response in the same assay (**Supplementary Fig. 4a**,**b**). Both compounds were confirmed to bind and inhibit USP10 in mutant-FLT3-expressing cells via competitive activity-based protein profiling[20] and evaluation of the protein levels of a known USP10 substrate, Beclin-1 (ref. 21). USP10 in lysates from live cells treated with either inhibitor was blocked from being labeled with a hemagglutinin (HA)-tagged ubiquitin probe modified to covalently label the active site cysteine of DUBs (HA-Ub-VS) with inhibitor concentrations in the low micromolar range (**Fig. 3a**,**b**). In addition, amounts of Beclin-1 and FLT3 were strongly decreased in FLT3-ITD-expressing Ba/F3 and MOLM14 cells treated with 20 μM HBX19818 (**Fig. 3c**,**d**). Beclin-1 levels, like FLT3 levels, were also strongly decreased in MOLM14 cells treated with 10 μM P22077 (**Fig. 3e**), and the protein was partially degraded in FLT3-ITD-expressing Ba/F3 cells (**Supplementary Fig. 4c**). We note that although they have been validated only as USP10 and USP7 inhibitors, both compounds exhibited at least some degree of inhibitory activity against other DUBs, and potentially against non-DUB targets, which probably contributed to the antiproliferative effects observed at concentrations below the point at which USP10 was well inhibited by the compounds.

USP10 has been reported to regulate the localization and stability of the tumor suppressor p53 (ref. 22). Because a drug that degrades wild-type p53 could be undesirable, we sought to determine whether pharmacological USP10 inhibition affects p53 levels in AML cell lines that express the transcription factor. Treatment of MOLM13-luc+ and MOLM14 cells with HBX19818 or P22077 did not result in decreased p53 levels; in fact, if anything, a modest increase in p53 levels was observed (**Supplementary Fig. 3a**,**b**). USP10 knockdown with short hairpin RNA (shRNA) did, as expected, result in decreased amounts of p53. HBX19818 and P22077 were both originally reported as USP7 inhibitors[18,20]. USP7 stabilizes MDM2, leading to increased ubiquitination and degradation of p53. It has been shown that pharmacological USP7 inhibition decreases MDM2 levels and increases p53 levels[19]. The USP7-inhibitory activity of the inhibitors may counteract any potential effects on p53 degradation by USP10.

As a first assessment of a potential role for USP10 in FLT3-mutant AML, we evaluated a small series of HBX19818 analogs for inhibitory activity toward USP10 in a biochemical assay, effects

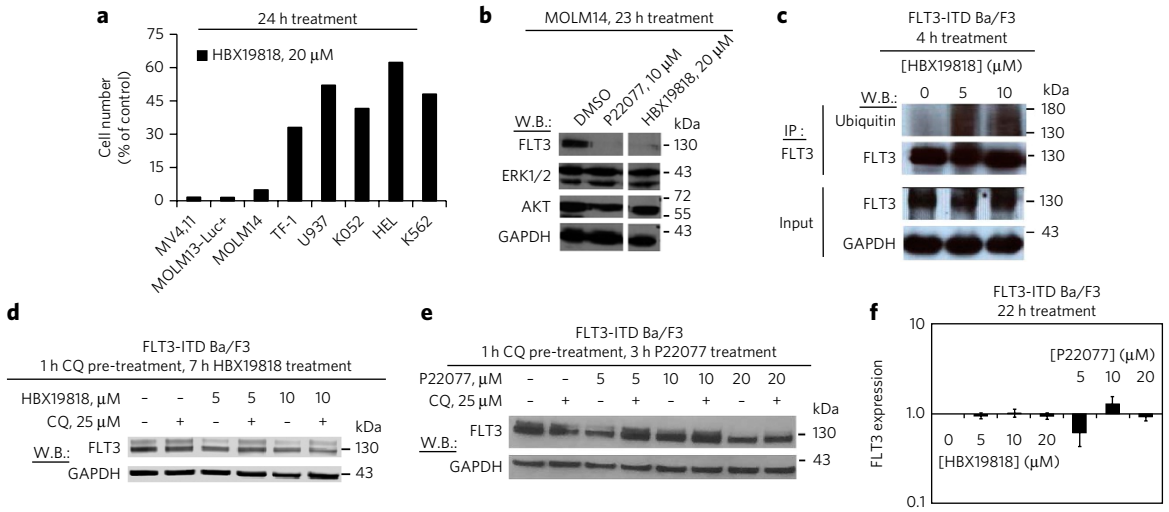

Figure 2 | Targeted and selective effects of HBX19818 and P22077 on mutant-FLT3-expressing human AML cells and investigation of the mechanism of ubiquitin-mediated degradation. (**a**) Analysis of the proliferation of mutant-FLT3-positive MV4;11, MOLM13-luc+ and MOLM14 cells as compared with leukemia cells expressing no or wild-type FLT3 after 24 h of treatment with 20 μM HBX19818 ($n = 2$). (**b**) Analysis of FLT3, ERK1/2 and AKT expression in MOLM14 cells treated with P22077 or HBX19818 for approximately 23 h. The full immunoblot is shown in **Supplementary Figure 4l**. This immunoblot is representative of three independent experiments that yielded similar results. (**c**) The effect of HBX19818 on the ubiquitination of mutant FLT3. This immunoblot is representative of four independent experiments for which similar results were observed. IP, immunoprecipitation. (**d**,**e**) Rescue of FLT3 degradation in HBX19818-treated (**d**) and P22077-treated (**e**) FLT3-ITD-expressing Ba/F3 cells by the lysosome inhibitor chloroquine (CQ). The results shown are representative of experiments performed in duplicate for which similar results were observed. (**f**) The effects of HBX19818 and P22077 on FLT3 transcription in FLT3-ITD-expressing Ba/F3 cells after 22 h of treatment. FLT3 expression is shown relative to GAPDH expression. The data represent the mean ± s.d. of $n = 3$ independent experiments.

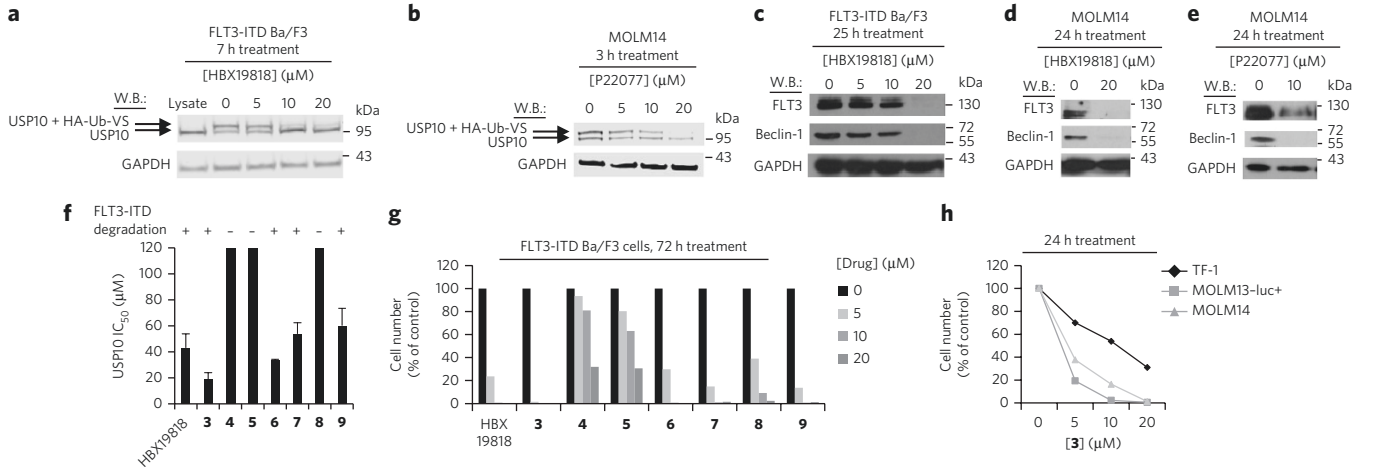

Figure 3 | Investigation of DUB targets of HBX19818 and P22077. (**a**,**b**) Target engagement studies: FLT3-ITD-expressing Ba/F3 cells and MOLM14 cells were treated with the indicated concentrations of compound, lysed, and incubated with 0.25 μg HA-Ub-VS for 30 min at room temperature. The ability of a compound to block USP10 labeling by HA-Ub-VS indicated binding of the enzyme by the inhibitor. These data are representative of at least two independent experiments for which similar results were observed. (**c**–**e**) Analysis of FLT3 and Beclin-1 levels in HBX19818-treated (**c**,**d**) and P22077-treated (**e**) FLT3-ITD-expressing Ba/F3 cells (**c**) and MOLM14 cells (**d**,**e**). (**f**) USP10 biochemical IC_{50} values for HBX19818 and HBX19818 analogs, with Ub-AMC used as the substrate. The ability of each compound to promote the loss of FLT3 is indicated by + or −. These data are representative of two independent experiments for which similar results were observed ($n = 2$). Error bars represent the s.d. (**g**) The effects of HBX19818 and structural analogs of HBX19818 on the proliferation of FLT3-ITD-expressing Ba/F3 cells after ~72 h of treatment ($n = 2$). (**h**) Analysis of the proliferation of FLT3-null TF-1 cells compared with that of FLT3-ITD-expressing MOLM13-luc+ and MOLM14 cells after 24 h of treatment with **3** at 0, 5, 10 and 20 μM concentrations ($n = 2$).

on FLT3 protein levels, and antiproliferative effects against Ba/F3 cells expressing FLT3-ITD (chemical structures are shown in **Supplementary Fig. 4d**). We observed good correlation among these parameters, supporting the idea that USP10 is the relevant target of HBX19818 (**Fig. 3f**,**g** and **Supplementary Fig. 4e–k**). For example, **9**, which inhibited USP10 similarly to HBX19818 (**Fig. 3f**) but did not inhibit USP7 (IC_{50} >> 100 μM; **Supplementary Table 3**), suppressed cell growth and induced a loss of FLT3 at similar concentrations (**Fig. 3g**, **Supplementary Fig. 4k**). The more potent USP10 inhibitor **3** (**Fig. 3f**) had a lower antiproliferation EC_{50} and induced FLT3 degradation at lower concentrations compared with HBX19818 (**Fig. 3g**, **Supplementary Fig. 4e**), whereas 4 showed little inhibition of USP10 in a purified enzyme assay (IC_{50} >>100 μM; **Fig. 3f**), a considerably right-shifted antiproliferation curve and no effect on FLT3 levels at the same concentrations at which HBX19818 degraded FLT3 (**Fig. 3g**, **Supplementary Fig. 4f**). The more potent HBX19818 analog, **3**, maintained specificity for FLT3-mutant MOLM13-luc+, MOLM14 and MV4,11 cell lines relative to the FLT3-null TF-1 cell line and to other leukemia lines not driven by FLT3 (**Fig. 3h**, **Supplementary Table 2**), and led to a loss in cell-surface FLT3 expression (**Supplementary Fig. 1d**). Also similarly to HBX19818, two analogs, **7** and **9**, primed mutant-FLT3-expressing cells more strongly than they did cells expressing wild-type or no FLT3 (**Supplementary Fig. 2h–i**).

USP10 knockdown and overexpression studies

Having identified USP10 as the prime candidate for involvement in mutant-FLT3 degradation by HBX19818 and P22077, we further investigated its role in FLT3-mutant AML via knockdown with three separate shRNAs targeting each DUB. USP10 knockdown with each shRNA resulted in the robust degradation of FLT3-ITD, as well as substantial growth inhibition in FLT3-ITD-positive cells (MOLM13-luc+ and MOLM14), as compared with treatment with the scrambled control shRNA (**Fig. 4a–c**, **Supplementary Fig. 5a**,**b**). As was observed for treatment with HBX19818 and P22077, USP10 knockdown had little to no effect on signaling molecules downstream of FLT3, including AKT and ERK1/2 (**Fig. 4c**). Effective USP10 knockdown by the same shRNAs did not suppress the growth of transformed human hematopoietic cell lines not driven by oncogenic FLT3 (K052, K562, KU812F and U937) (**Fig. 4a**, **Supplementary Fig. 5c–f**) and, similar to USP10-targeted small-molecule inhibition, did not modulate levels of wild-type FLT3 (**Fig. 4d**,**e**, **Supplementary Fig. 5c–e**). In addition, we observed that levels of USP10 were generally higher in most cell lines that expressed higher levels of FLT3, including MOLM14 and MV4,11, consistent with a stabilizing role for USP10 in the regulation of FLT3 (**Supplementary Fig. 5g**). In contrast to the results of USP10 knockdown, we observed little to no change in levels of FLT3 or Beclin-1 in FLT3-ITD-expressing MOLM14 cells after USP7 knockdown (**Supplementary Fig. 6a**), and transduction with the USP7-targeting shRNAs had little to no effect on cell viability compared with treatment with the scrambled control shRNA (**Supplementary Fig. 6b**). USP7 knockdown was demonstrated to be selective, as levels of USP10 decreased in USP10-knockdown cells but remained unchanged in USP7-knockdown cells (**Supplementary Fig. 6c**,**d**). Furthermore, pharmacological inhibition of USP7 with the selective USP7 inhibitor USP7i-1 (ref. 23) had less of an effect than HBX19818 had on cell viability and did not lead to reduced FLT3 levels in FLT3-ITD-expressing Ba/F3 cells at concentrations up to 20 μM (**Supplementary Fig. 6e–g**).

In the converse experiment, we observed that increased expression of USP10 correlated with higher stabilization of FLT3-ITD than of wild-type FLT3 in stably transfected MOLM14 cells and transiently transfected HEK293T cells (**Fig. 4f**, **Supplementary Fig. 7a**,**b**). We note that, similar to their effects in oncogenic-FLT3-driven AML cells, both HBX19818 and P22077 were able to induce the degradation of FLT3 in HEK293T cells, although approximately twofold-higher concentrations were needed to replicate the effects observed with both compounds in mutant-FLT3-driven cells (**Supplementary Fig. 7c**). The introduction of USP10 in which the catalytic cysteine was replaced with serine (USP10C424S) into MOLM14 cells resulted in reduced stabilization of mutant FLT3 compared with that of the wild-type protein, confirming the importance of USP10's catalytic activity in regulating FLT3-ITD protein levels (**Fig. 4f**). Taken together, the result of our structure–activity relationship, knockdown and overexpression studies strongly

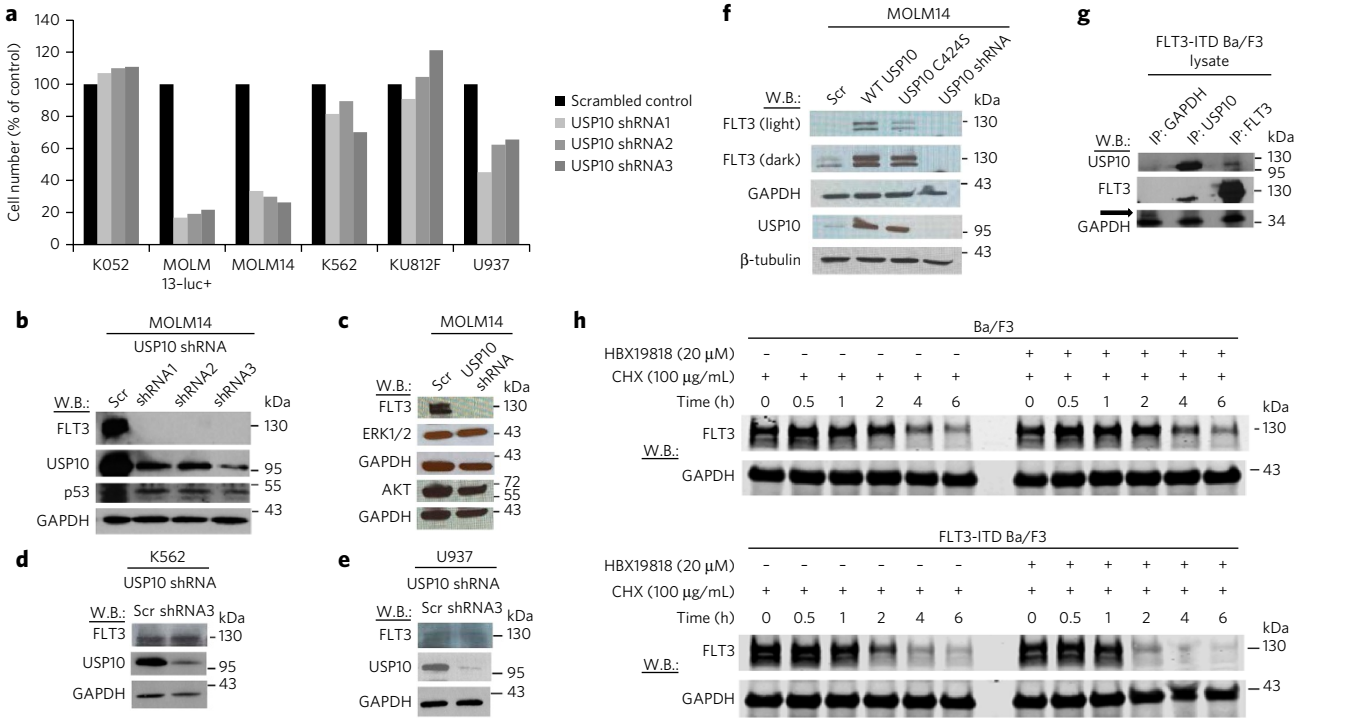

Figure 4 | Investigation of USP10 as a mediator of FLT3-ITD and wild-type FLT3. (**a**) Cell counts (based on trypan blue exclusion assay) determined approximately 1 week after puromycin selection of USP10 shRNA–infected cells ($n = 2$). (**b**) The effects of USP10 knockdown on FLT3 and p53 protein levels in MOLM14 cells. (**c**) The effects of USP10 knockdown on FLT3, AKT and ERK1/2 protein levels in MOLM14 cells. (**d**,**e**) The effects of USP10 knockdown on FLT3 expression in K562 (**d**) and U937 (**e**) cells expressing wild-type FLT3. The immunoblots shown in **b**–**e** are representative of at least two experiments for which similar results were observed. (**f**) Analysis of FLT3 levels in MOLM14 cells overexpressing wild-type USP10 and catalytically inactive USP10 (USP10C424S). The immunoblot shown is representative of three experiments for which similar results were observed (**Supplementary Fig. 7a**). (**g**) The association of endogenous USP10 with exogenously expressed FLT3-ITD in FLT3-ITD-expressing Ba/F3 cells. The GAPDH IP served as a control. The arrow is pointing to GAPDH; the lower bands observed are probably the IgG light chain associated with the IP ($n = 1$). Results were replicated with exogenously expressed proteins (**Supplementary Fig. 7d**). (**h**) HBX19818 shortened the half-life of FLT3-ITD (bottom) to a greater extent than that of wild-type FLT3 (top). These data are representative of three independent experiments for which similar results were observed (**Supplementary Fig. 8**). Scr, scrambled shRNA; CHX, cycloheximide.

support the theory that USP10 is the critical regulator of FLT3-ITD stability; however, they do not address whether this effect is direct or indirect. To answer this, we examined whether USP10 and FLT3 are in a complex in cells that express mutant FLT3. We observed robust co-immunoprecipitation of USP10 with FLT3 in FLT3-ITD-expressing Ba/F3 cells; reverse co-immunoprecipitation studies confirmed the association of FLT3 with USP10 (**Fig. 4g**). We found a similar interaction between USP10 and FLT3 in HEK293T cells engineered to exogenously express these proteins (**Supplementary Fig. 7d**). We observed that HBX19818 at 2, 4 and 6 h and the chemokine P22077 at 4 and 6 h blocked the interaction between USP10 and FLT3-ITD (**Supplementary Fig. 7e**).

USP10 stabilizes FLT3-ITD more than wild-type FLT3

The observed differential effects on wild-type and mutant forms of FLT3 with USP10 pharmacological inhibition and knockdown, as well as enzyme overexpression, are in agreement with reports that activated FLT3 is more prone to ubiquitin-mediated degradation[15]. We analyzed the half-lives of wild-type FLT3 and FLT3-ITD with and without overexpression of USP10 and in the absence and presence of HBX19818 to see whether differences in protein stability might play a role in the differential responsiveness of the two proteins to DUB-inhibitor treatment. In Ba/F3 cells, HBX19818 shortened the half-life of FLT3-ITD from 3–4 h to around 2 h, and shortened the half-life of FLT3-ITD to a greater extent than it did that of wild-type FLT3 (**Fig. 4h**, **Supplementary Fig. 8**). The data suggest that this differential responsiveness to HBX19818 between wild-type FLT3 and FLT3-ITD might be due to modest differences in the inherent overall stability or half-lives of these proteins.

Degradation of mutant FLT3 overcomes resistance

We sought to confirm that ubiquitin-mediated degradation could be advantageous compared with FLT3 kinase inhibition in terms of the ability to override drug resistance. Treatment of Ba/F3 cells expressing both FLT3-ITD and TKD point mutations with the FLT3 kinase inhibitors led to rightward shifts in the dose–response curves (**Fig. 5a**, **Supplementary Fig. 9a**,**b**), validating previous reports of differential resistance to these inhibitors. In contrast, HBX19818 and P22077 treatments were equipotent against FLT3-ITD-expressing Ba/F3 cells with and without the TKD point mutations, but less potent toward Ba/F3 cells engineered to overexpress wild-type FLT3 (**Fig. 5b**,**c**). HBX19818 and P22077 induced the degradation of FLT3 in cells resistant to FLT3 kinase inhibitor at concentrations that were ineffective in promoting FLT3 degradation in Ba/F3 cells expressing wild-type FLT3 (**Figs. 1f** and **5d**,**e**, **Supplementary Figs. 1e** and **9c–f**). All TKD point mutants were confirmed to express constitutively activated FLT3 (**Supplementary Fig. 9g**,**h**). In addition, HBX19818 and P22077 showed similar potency toward parental MOLM13 cells and MOLM13 cells rendered resistant to the FLT3 kinase inhibitor midostaurin after prolonged culture in the presence of the drug (**Fig. 5f–h**). Midostaurin-resistant MOLM13 cells have been characterized as having high overexpression of FLT3, which is believed to contribute to their resistance[24].

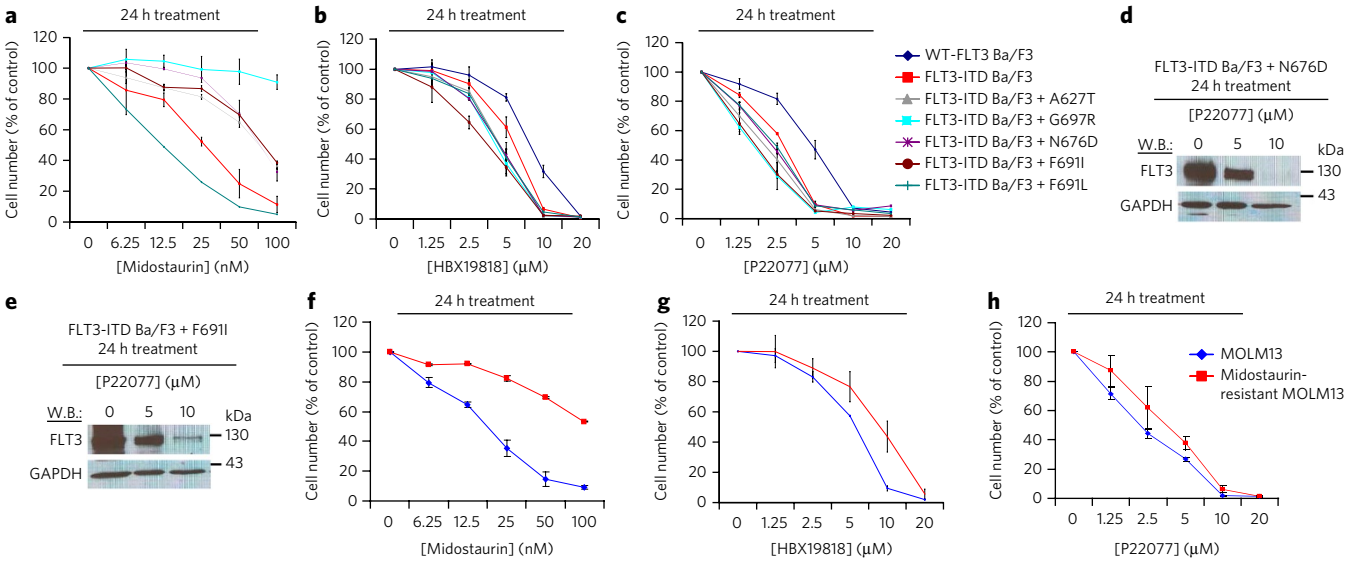

Figure 5 | Targeted effects of HBX19818 and P22077 on cells resistant to FLT3 kinase inhibitors. (**a**–**c**) Ba/F3 cells expressing wild-type FLT3, FLT3-ITD or FLT3-ITD plus TKD point mutations after ~24 h of treatment with midostaurin (**a**), HBX19818 (**b**) or P22077 (**c**) ($n = 2$). (**d**,**e**) Effects of HBX19818 and P22077 on FLT3 expression in FLT3-ITD-expressing Ba/F3 cells with the indicated TKD point mutations after 24 h of treatment. Immunoblotting was performed once. (**f**–**h**) Comparison of the effects of midostaurin (**f**), HBX19818 (**g**) and P22077 (**h**) on the proliferation of MOLM13 cells and midostaurin-resistant MOLM13 cells ($n = 2$). Error bars in **a**–**c**,**f**–**h** indicate ±s.d.

HBX19818 acts synergistically with FLT3 kinase inhibitors

To further assess the therapeutic potential of USP10 inhibition, we investigated the ability of DUB inhibitors and FLT3 kinase inhibitors to interact synergistically. Specifically, we used a median-drug-effect analysis in which we calculated a combination index (CI) from growth-inhibition curves using Calcusyn software (Biosoft, Cambridge, UK). Dual treatment of FLT3-ITD-expressing Ba/F3 cells, MOLM13-luc+ cells and MOLM14 cells with HBX19818 and FLT3 kinase inhibitor (midostaurin or crenolanib) at a fixed-ratio serial dilution resulted in decreased cell growth compared with treatment with either agent alone (**Supplementary Fig. 9i–k**). CI analysis indicated synergistic antiproliferative effects (values less than 1 indicate synergy) at 25%, 50%, 75% and 90% growth inhibition for MOLM13-luc+ cells and FLT3-ITD-expressing Ba/F3 cells, and at 50%, 75% and 90% growth inhibition for MOLM14 cells (**Fig. 6a**,**b**, **Supplementary Fig. 9l**) after concomitant treatment with either kinase inhibitor and HBX19818.

Targeting FLT3 is efficacious in AML preclinical models

We next evaluated the therapeutic potential of our lead USP10 inhibitor series by testing their growth-inhibitory effects on primary patient tumor samples and patient-derived xenografts (PDXs; also known as primagrafts) *ex vivo*. USP10 inhibitors HBX19818 and P22077 and selected HBX19818 analogs all caused a dose-dependent reduction in survival in two each of FLT3-ITD-positive patient samples and PDXs (**Fig. 6c–e**, **Supplementary Fig. 10a–d**). HBX19818 was less potent toward two donor peripheral blood mononucleated cell (PBMC) samples from healthy donors, and P22077 was less potent toward one of two PBMC samples it was tested against (**Fig. 6e**, **Supplementary Fig. 10d**, **Supplementary Tables 4–7**). The selective USP7 inhibitor USP7i-1 had little to no effect on the survival of these samples (**Fig. 6c**,**d**, **Supplementary Fig. 10a**,**c**). We obtained enough cells from one PDX to analyze FLT3 levels via immunoblotting, and the results indicated a strong reduction in the amount of FLT3 after 21 h of treatment with either HBX19818 or P22077 at a concentration of 20 μM (**Supplementary Fig. 10e**).

These results inspired us to test P22077 *in vivo*, using the same FLT3-ITD$^+$ and FLT3-D835Y$^+$ AML primagraft in which P22077 induced FLT3 degradation *ex vivo*. Following the methodology for *in vivo* administration of P22077 outlined in ref. 25, we administered vehicle (10% DMSO, 90% D5W (vol/vol)) ($n = 3$) or P22077 (15 mg/kg body weight) ($n = 3$) to primagraft-recipient mice intraperitoneally once per day after disease was detected by flow cytometry. Immunoblot analysis of protein lysates from mouse bone marrow cells, collected after 21 d of treatment and pooled respectively from each treatment group, showed a strong FLT3 signal in vehicle-treated mice that was undetectable in P22077-treated mice (**Supplementary Fig. 10f**), suggesting drug-induced FLT3 degradation *in vivo*. We note that the mice generally tolerated 15 mg/kg P22077 well over the course of the 21-d treatment period, with little change in weight (approximately 2–3 g of weight lost on average in both vehicle-treated and P22077-treated mice; none of the mice lost more than 15% of their body weight).

We also tested the ability of P22077 to suppress the growth of mutant-FLT3-positive cells in a second model, a non-invasive *in vivo* bioluminescence model. First we confirmed that Ba/F3 cells that co-expressed FLT3-ITD and luciferase (FLT3-ITD–luc+) responded to midostaurin and P22077 similarly to non-luciferase-expressing cells in terms of growth suppression and FLT3 degradation (**Supplementary Fig. 10g–j**) and DUB-inhibitor-induced loss of surface FLT3 expression (**Supplementary Fig. 10k**). In a small pilot study, we treated female NCR nude mice harboring FLT3-ITD–luc+ Ba/F3 cells with 50 mg/kg P22077 twice daily via intraperitoneal injection ($n = 4$) for 4 d. At the end of the treatment period, bone marrow from P22077-treated mice showed approximately twofold lower FLT3 expression compared with that in bone marrow extracted from vehicle-treated mice ($n = 4$), as measured by flow cytometry with a phycoerythrin (PE)-conjugated antibody to CD35 (**Fig. 6f**). Aliquots of the bone marrow samples showed a similar (approximately twofold) reduction in luciferase signal in P22077-treated mouse bone marrow samples compared with that in controls (**Fig. 6f**). Taken together, these results suggest a reduction in tumor burden via on-target effects. We then carried out a larger, three-arm ($n = 8$ per arm) study in which we administered 50 mg/kg P22077 twice daily via intraperitoneal injection, P22077 once daily via oral gavage, or vehicle to female NCR nude mice harboring FLT3-ITD–luc+ Ba/F3 cells. P22077 treatment led to the

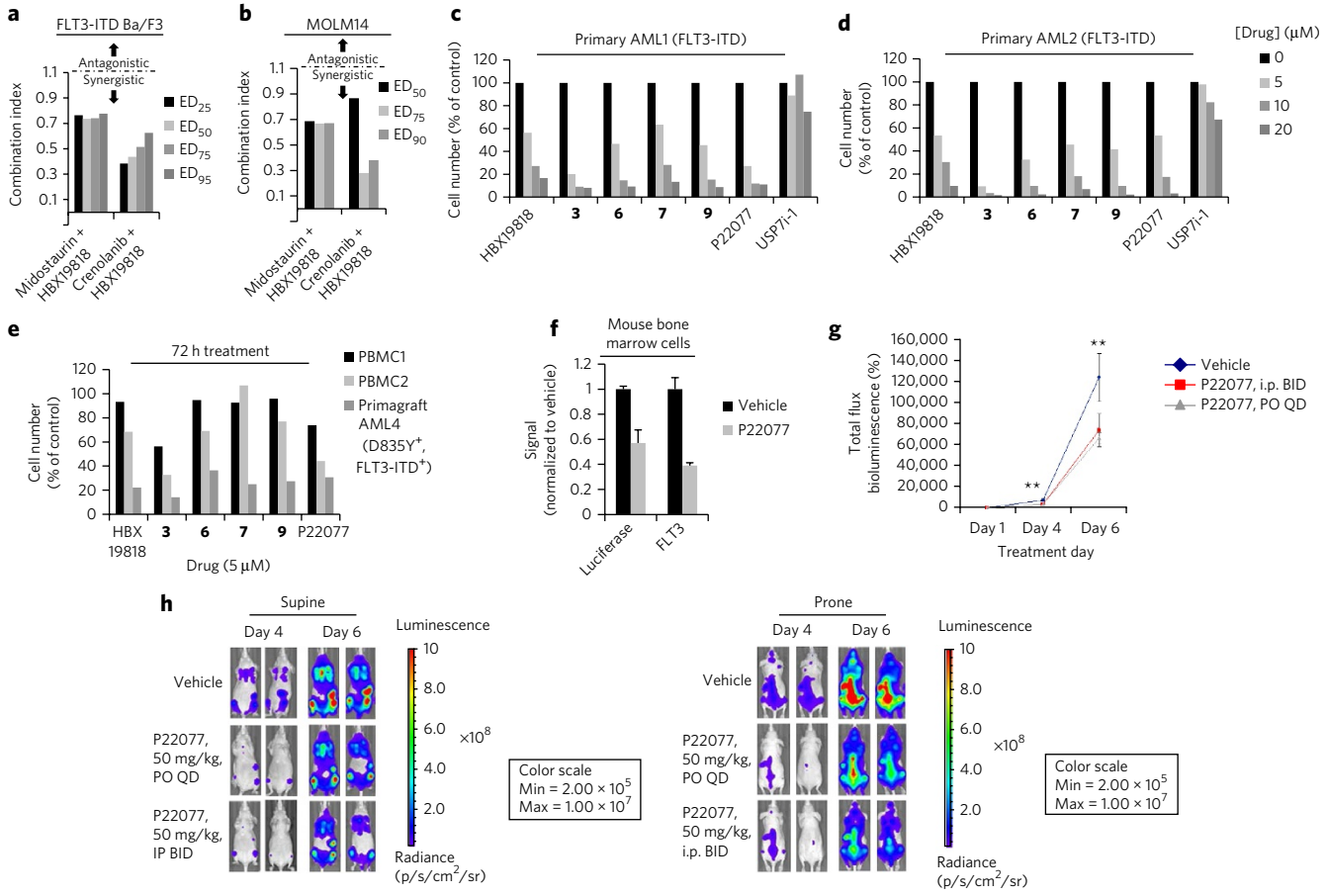

Figure 6 | Effects of the combination of HBX19818 with FLT3 kinase inhibitors and targeted effects of USP10 inhibition on mutant-FLT3-positive AML primary cells *in vitro* and *in vivo*. (**a**) Combination indices corresponding to co-treatment of FLT3-ITD-expressing Ba/F3 cells with HBX19818 and either midostaurin or crenolanib ($n = 2$). (**b**) Combination indices corresponding to co-treatment of MOLM14 cells with HBX19818 and either midostaurin or crenolanib ($n = 2$). (**c**,**d**) Effects of DUB inhibitors on FLT3-ITD-expressing primary cells from patients with AML1 (**c**) or AML2 (**d**) after ~72 h of treatment ($n = 2$). (**e**) The effects of USP10 inhibitors on normal PBMCs and on mutant-FLT3-expressing AML primagraft cells (D835Y$^+$FLT3-ITD$^+$) after 72 h of treatment ($n = 2$). (**f**) The correlation between luciferase-positive leukemia burden, as measured by Bright Glo assay and luminoskan, and the percentage of FLT3, as measured by flow cytometry with a PE-conjugated antibody to CD135, in bone marrow samples from vehicle- versus P22077 (50 mg/kg i.p. twice a day)-treated mice (pilot study; 4-d treatments) ($n = 3$). (**g**,**h**) The effects of P22077 treatment on the growth of FLT3-ITD–luc+ Ba/F3 cells in a non-invasive *in vivo* bioluminescence model of leukemia ($n = 7$–8). (**g**) Total flux bioluminescence. BID, twice-daily dose; PO QD, once-daily oral dose. (**h**) Bioluminescence images of representative mice with matched starting leukemia burdens. Student's *t*-test (two-sided): vehicle versus twice-daily i.p. P22077 on day 4 ($P = 0.0069212$) and day 6 ($P = 0.1033934$); vehicle versus oral once-daily P22077 on day 4 ($P = 0.0034501$) and day 6 ($P = 0.0425383$). **Statistically significant. Error bars in **f** and **g** represent the s.e.m.

death of FLT3-ITD-expressing cells *in vivo* as measured by *in vivo* bioluminescence, with a statistically significant decrease in leukemia burden compared with that in vehicle-treated mice after 4–6 d of treatment (**Fig. 6g**,**h**). We did not observe any significant difference in weight between vehicle- and drug-treated mice after up to 11 d of treatment (**Supplementary Fig. 10l**,**m**). There was also generally no evidence of vital organ toxicity in the mice.

DISCUSSION

The 5-year survival rate for AML patients is only 20% (ref. 26). The prognosis is especially poor for patients who harbor FLT3-ITD mutations, as these are associated with aggressive and lethal disease[27]. Treatment with FLT3 kinase inhibitors unfortunately provides responses of only short duration as a result of eventual drug resistance[28]. Additionally, patients treated with FLT3 kinase inhibitors may experience side effects such as myelosuppression due to the inhibition of wild-type FLT3 (ref. 29). These limitations warrant the development of novel, targeted agents. Therapeutic targeting of mutant FLT3 via promotion of its degradation, as opposed to inhibition of its kinase activity, is a novel approach that may be beneficial for overcoming resistance to current FLT3 kinase inhibitors and prove more efficacious than kinase inhibitors by simultaneously blocking both enzymatic and scaffolding functions of FLT3.

Here we introduce the DUB USP10 as a critical effector enzyme of tumor growth and survival in subjects with FLT3-ITD-positive AML, and we present two chemical classes of USP10 inhibitor that were observed to promote FLT3 degradation and confer an antiproliferative effect *in vitro* and *in vivo*. Most studies aimed at the identification of the DUB responsible for the stabilization of a substrate of interest start with a genetic-based screen—typically involving knockdown or overexpression of individual DUBs—that measures protein levels. We, however, applied an approach that is frequently used in the kinase field but, to the best of our knowledge, has not yet been reported in the DUB field and screened small-molecule DUB inhibitors for their ability to selectively suppress the growth of mutant-FLT3-expressing cells versus cells expressing wild-type FLT3. This strategy was enabled by our assembly of a DUB-inhibitor library and annotation of the library for inhibitory activity across a large panel of DUBs. The top hit from our screen, HBX19818, led to striking and selective antiproliferative effects against mutant-FLT3-positive

cells resulting from the inhibition of USP10, a previously unreported target of the compound. Our small-molecule-centered approach enabled us to not only identify a novel mechanism for the regulation of FLT3-ITD but also rapidly interrogate the translational potential of pharmacological inhibition of USP10 in mutant-FLT3-driven AML in preclinical models. The data generated across multiple models strongly support the notion that USP10 inhibition may offer a novel strategy for targeting mutant-FLT3 AML clinically and has the potential to overcome kinase-inhibitor-resistance mechanisms.

The observed selective degradation of mutant FLT3 might allow therapies that spare wild-type FLT3 in normal hematopoietic cells, and thus offer a substantial clinical advantage over FLT3 kinase inhibitors that inhibit both wild-type and mutant enzyme. Phosphorylation of the FLT3 receptor is necessary for FLT3 ubiquitination and degradation by the E3 ubiquitin ligase CBL[16,30], and both we and others have observed more phosphorylation of mutant FLT3 than of wild-type FLT3 in the absence of FLT3 ligand, with the highest levels of autophosphorylation observed in cells that expressed both FLT3-ITD and TKD mutations. Experimentally, we observed that the half-life of FLT3-ITD after HBX19818 treatment was shorter than that of wild-type FLT3. Our data support previous reports that autophosphorylated FLT3-ITD, as compared with wild-type FLT3, undergoes more rapid degradation via proteasome- and lysosome-mediated pathways, with degradation facilitated by the E3 ubiquitin ligases c-Cbl and Cbl-b[15]. Together, these data suggest that mutant FLT3 exists in a state more prone to ubiquitination than wild-type FLT3, and this may account for our observed selective degradation of mutant FLT3 versus wild-type FLT3 in the presence of USP10 inhibition.

These are early but exciting days for the DUB-inhibitor field. Approximately 40 DUB inhibitors have been reported. Although the majority exhibit modest potency (micromolar range) and are polypharmacological agents[9], recent reports of potent and selective inhibitors lend confidence to the notion that high-quality probes and lead therapeutics targeting the gene family can be generated in significant numbers[31,32]. As an increasing number of papers implicate DUBs in disease, efforts are also increasing to identify novel inhibitors. We believe that with the development of DUB-targeting libraries, stringent compound triaging after high-throughput screening, and success in crystallography enabling structure-guided medicinal chemistry efforts, novel probes are on the horizon.

Overall, these findings indicate that therapeutic targeting of USP10 has potent suppressive effects on FLT3-ITD-positive AML, including forms that involve kinase-inhibitor-resistant FLT3 mutants. This novel approach warrants further investigation as an alternative treatment strategy for this disease. We are currently applying the same screening approach to other mutant proteins that help drive AML in subsets of patients.

Received 29 December 2016; accepted 25 August 2017;
published online 2 October 2017

METHODS

Methods, including statements of data availability and any associated accession codes and references, are available in the online version of the paper.

References

1. Hershko, A. The ubiquitin system for protein degradation and some of its roles in the control of the cell division cycle. *Cell Death Differ.* **12**, 1191–1197 (2005).
2. Clague, M.J., Coulson, J.M. & Urbé, S. Cellular functions of the DUBs. *J. Cell Sci.* **125**, 277–286 (2012).
3. Pickart, C.M. & Fushman, D. Polyubiquitin chains: polymeric protein signals. *Curr. Opin. Chem. Biol.* **8**, 610–616 (2004).
4. Heideker, J. & Wertz, I.E. DUBs, the regulation of cell identity and disease. *Biochem. J.* **465**, 1–26 (2015).
5. Clague, M.J. *et al.* Deubiquitylases from genes to organism. *Physiol. Rev.* **93**, 1289–1315 (2013).
6. Abdul Rehman, S.A. *et al.* MINDY-1 is a member of an evolutionarily conserved and structurally distinct new family of deubiquitinating enzymes. *Mol. Cell* **63**, 146–155 (2016).
7. Sowa, M.E., Bennett, E.J., Gygi, S.P. & Harper, J.W. Defining the human deubiquitinating enzyme interaction landscape. *Cell* **138**, 389–403 (2009).
8. Williams, S.A. *et al.* USP1 deubiquitinates ID proteins to preserve a mesenchymal stem cell program in osteosarcoma. *Cell* **146**, 918–930 (2011).
9. Ndubaku, C. & Tsui, V. Inhibiting the deubiquitinating enzymes (DUBs). *J. Med. Chem.* **58**, 1581–1595 (2015).
10. Atwal, R.S. *et al.* Kinase inhibitors modulate huntingtin cell localization and toxicity. *Nat. Chem. Biol.* **7**, 453–460 (2011).
11. Li, Z. & Rana, T.M. A kinase inhibitor screen identifies small-molecule enhancers of reprogramming and iPS cell generation. *Nat. Commun.* **3**, 1085 (2012).
12. Levis, M. *FLT3* mutations in acute myeloid leukemia: what is the best approach in 2013? *Hematology (Am. Soc. Hematol. Educ. Program)* **2013**, 220–226 (2013).
13. Weisberg, E. *et al.* FLT3 inhibition and mechanisms of drug resistance in mutant FLT3-positive AML. *Drug Resist. Updat.* **12**, 81–89 (2009).
14. Stone, R.M. *et al.* Midostaurin plus chemotherapy for acute myeloid leukemia with a *FLT3* mutation. *N. Engl. J. Med.* **377**, 454–464 (2017).
15. Oshikawa, G., Nagao, T., Wu, N., Kurosu, T. & Miura, O. c-Cbl and Cbl-b ligases mediate 17-allylaminodemethoxygeldanamycin-induced degradation of autophosphorylated Flt3 kinase with internal tandem duplication through the ubiquitin proteasome pathway. *J. Biol. Chem.* **286**, 30263–30273 (2011).
16. Sargin, B. *et al.* Flt3-dependent transformation by inactivating c-Cbl mutations in AML. *Blood* **110**, 1004–1012 (2007).
17. Ritorto, M.S. *et al.* Screening of DUB activity and specificity by MALDI-TOF mass spectrometry. *Nat. Commun.* **5**, 4763 (2014).
18. Reverdy, C. *et al.* Discovery of specific inhibitors of human USP7/HAUSP deubiquitinating enzyme. *Chem. Biol.* **19**, 467–477 (2012).
19. Chauhan, D. *et al.* A small molecule inhibitor of ubiquitin-specific protease-7 induces apoptosis in multiple myeloma cells and overcomes bortezomib resistance. *Cancer Cell* **22**, 345–358 (2012).
20. Altun, M. *et al.* Activity-based chemical proteomics accelerates inhibitor development for deubiquitylating enzymes. *Chem. Biol.* **18**, 1401–1412 (2011).
21. Liu, J. *et al.* Beclin1 controls the levels of p53 by regulating the deubiquitination activity of USP10 and USP13. *Cell* **147**, 223–234 (2011).
22. Yuan, J., Luo, K., Zhang, L., Cheville, J.C. & Lou, Z. USP10 regulates p53 localization and stability by deubiquitinating p53. *Cell* **140**, 384–396 (2010).
23. Kessler, B.M. Selective and reversible inhibitors of ubiquitin-specific protease 7: a patent evaluation (WO2013030218). *Expert Opin. Ther. Pat.* **24**, 597–602 (2014).
24. Weisberg, E. *et al.* Reversible resistance induced by FLT3 inhibition: a novel resistance mechanism in mutant FLT3-expressing cells. *PLoS One* **6**, e25351 (2011).
25. Fan, Y.H. *et al.* USP7 inhibitor P22077 inhibits neuroblastoma growth via inducing p53-mediated apoptosis. *Cell Death Dis.* **4**, e867 (2013).
26. De Kouchkovsky, I. & Abdul-Hay, M. Acute myeloid leukemia: a comprehensive review and 2016 update. *Blood Cancer J.* **6**, e441 (2016).
27. Martelli, M.P., Sportoletti, P., Tiacci, E., Martelli, M.F. & Falini, B. Mutational landscape of AML with normal cytogenetics: biological and clinical implications. *Blood Rev.* **27**, 13–22 (2013).
28. Weisberg, E. *et al.* Discovery and characterization of novel mutant FLT3 kinase inhibitors. *Mol. Cancer Ther.* **9**, 2468–2477 (2010).
29. Warkentin, A.A. *et al.* Overcoming myelosuppression due to synthetic lethal toxicity for FLT3-targeted acute myeloid leukemia therapy. *eLife* **3**, 03445 (2014).
30. Lavagna-Sévenier, C., Marchetto, S., Birnbaum, D. & Rosnet, O. FLT3 signaling in hematopoietic cells involves CBL, SHC and an unknown P115 as prominent tyrosine-phosphorylated substrates. *Leukemia* **12**, 301–310 (1998).
31. Dexheimer, T.S. *et al.* Discovery of ML323 as a novel inhibitor of the USP1/UAF1 deubiquitinase complex. In *Probe Reports from the NIH Molecular Libraries Program [Internet]* (National Center for Biotechnology Information, 2010). Available at https://www.ncbi.nlm.nih.gov/books/NBK259186/.
32. Báez-Santos, Y.M., St John, S.E. & Mesecar, A.D. The SARS-coronavirus papain-like protease: structure, function and inhibition by designed antiviral compounds. *Antiviral Res.* **115**, 21–38 (2015).

Acknowledgments

We thank D. Ye and S. Walker for their assistance with assessment of luciferase expression indicative of leukemia cell burden in the bone marrow of mice via the Bright-Glo luciferase assay system (Promega, Madison, Wisconsin, USA). Nomo-1, P31-FUJ and NB4 were obtained from G. Gilliland (Fred Hutchinson Cancer Research Center, Seattle, Washington, USA). MV4,11 cells were obtained from A. Letai (Dana-Farber Cancer Institute, Boston, Massachusetts, USA). The human FLT3-ITD-postive AML

line MOLM14 was obtained from S. Armstrong (Dana-Farber Cancer Institute, Boston, Massachusetts, USA). PBMCs were generously provided by S. Treon and G. Yang (Dana-Farber Cancer Institute, Boston, Massachusetts, USA). Flag-HA-USP10 was a gift from the Wade Harper lab (Harvard Medical School, Boston, Massachusetts, USA). Work was funded by the Dana-Farber Cancer Institute Accelerator Fund (S.J.B. and E.L.W.), the Leukemia and Lymphoma Society (S.J.B. and E.L.W.), the Chleck Family Foundation (N.J.S.), the National Science Fellowship Graduate Research Fellowship Program (L.D.) and the and Claudia Adams Barr Award (S.J.B. and E.L.W.).

Author contributions

E.L.W., S.J.B., N.S.G. and J.D.G. initiated the project, and E.L.W. and S.J.B. oversaw all aspects of the project. E.L.W., N.J.S., J.Y. and I.L. performed biochemical, proliferation, signaling, knockdown, overexpression and immunoprecipitation studies. S.B. and A.L. designed and performed mitochondrial priming experiments. A. Christie, A. Christodoulou and D.M.W. designed and performed primagraft studies. H.T. and P.C.G. designed and performed *in vivo* bioluminescence studies. M.S.R., V.D.C. and M.T. designed and performed MALDI-TOF DUB assays. S.A. performed flow cytometry experiments. A.N. performed gene-knockdown experiments. S.D.-P. and H.-S.S. were responsible for the generation of USP10 enzyme used in biochemical assays. L.D., C.M. and R.W. performed immunoblotting experiments. R.S. provided AML patient samples. M.S., D.C. and K.C.A. offered valuable scientific feedback and helped with the conception of the research reported in the paper. E.L.W. and S.J.B. wrote the manuscript with input from all other authors.

Competing financial interests

The authors declare no competing financial interests.

Additional information

Any supplementary information, chemical compound information and source data are available in the online version of the paper. Reprints and permissions information is available online at http://www.nature.com/reprints/index.html. Publisher's note: Springer Nature remains neutral with regard to jurisdictional claims in published maps and institutional affiliations. Correspondence and requests for materials should be addressed to E.L.W. or S.J.B.

ONLINE METHODS

Chemical compounds and biologic reagents. DUB inhibitors HBX19818 and P22077 were purchased from Medchem Express and dissolved in DMSO to produce a 10 mM stock solution. HBX19818 analogs were purchased from ChemDiv and dissolved in DMSO to produce a 10 mM stock solution. Results of UPLC-MS analysis for all compounds were in agreement with the reported purity and molecular weight. Serial dilutions were then made to produce final dilutions for cellular assays with a final concentration of DMSO not exceeding 0.1%.

Antibodies. The following antibodies were purchased from Cell Signaling Technology (Danvers, MA): total AKT (rabbit; 9272) and total p44/42 MAPK (Erk1/2) (3A7) (mouse; 9107) were used at 1:1,000. Anti-GAPDH (D16H-11) XP (R) (rabbit mAb; 5174) was used at 1:1,000. Beclin-1 (rabbit; 3738) was used at 1:1,000. USP10 (D7A5) (rabbit; 8501) was used at 1:1,000. P53 (rabbit; 9282) was used at 1:1,000. β-tubulin (rabbit; 2146s) was used 1:1,000.

FLT3/Flk-2 (C-20) (sc-479) and Ub (P4D1) (mouse; sc-8017) were purchased from Santa Cruz Biotechnology (Dallas, TX) and used at 1:1,000 for immunoblotting. Anti-pTyr (mouse; clone 4G10) was purchased from Upstate Biotechnology (Lake Placid, NY) and used at 1:1,000. Anti-HAUSP/USP7 (rabbit; ab4080) and anti-ubiquitin (rabbit; ab7780) were purchased from Abcam (Cambridge, MA) and used at 1:1,000.

Cell lines and cell culture. FLT3-ITD- or FLT3-D835Y-containing MSCV retroviruses were transfected into the mouse hematopoietic cell line Ba/F3 (IL-3-dependent) as previously described[33]. Nomo-1, P31-FUJ and NB4 were obtained from Dr. Gary Gilliland. MV4,11 cells were obtained from Dr. Anthony Letai. Hel, K562, THP, U937, TF-1 and K052 cells were purchased from the American Type Culture Collection (ATCC) (Manassas, VA, USA). The human FLT3-ITD-postive AML line MOLM14 (ref. 34) was obtained from Dr. Scott Armstrong, Dana-Farber Cancer Institute (DFCI), Boston, MA. The human FLT3-ITD-positive AML line MOLM-13 (DSMZ (German Resource Centre for Biological Material)) was made to express luciferase fused to neomycin phosphotransferase (pMMP-LucNeo) as previously described[35].

All cell lines were cultured at a concentration of 2×10^5 to 5×10^5 cells/mL in RPMI (Mediatech, Inc., Herndon, VA) with 10% FBS and supplemented with 2% L-glutamine and 1% penicillin–streptomycin. Exceptions included TF-1 and OCI-AML5 cells, which were cultured in RPMI media with 10% FBS and supplemented with 2% L-glutamine and 1% penicillin–streptomycin and human GM-CSF (2 ng/mL). Parental Ba/F3 cells were cultured in RPMI with 10% FBS and supplemented with 2% L-glutamine and 1% penicillin–streptomycin and 15–20% WEHI (as a source of IL-3). All cell lines were passaged in 5% CO_2 at 37 °C.

Cell lines used in this study were submitted for cell line authentication within 6 months of manuscript preparation by cell line short tandem repeat (STR) profiling (DDC Medical, Fairfield, OH, and Molecular Diagnostics Laboratory, Dana-Farber Cancer Institute). All cell lines matched ≥80% with lines listed in the ATCC or DSMZ Cell Line Bank STR and were confirmed to be virus- and mycoplasma-free.

PBMCs were generously provided by Dr. Steven Treon and Dr. Guang Yang.

Immunoblotting and immunoprecipitation. Preparation of protein lysates, immunoblotting and immunoprecipitation were carried out as described previously[36].

Proliferation studies. The trypan blue exclusion assay was used for quantification of cells before seeding for CellTiter-Glo Luminescent Cell Viability assays (Promega, Madison, WI) and carried out as described previously[36]. CellTiter-Glo luminescent cell viability assays, carried out according to the manufacturer's instructions, were used for proliferation studies. In the main text figures, cell viability is reported as a percentage of control (untreated) cells, and error bars represent the s.d. for each data point, unless stated otherwise.

AML patient cells. Mononuclear cells were isolated from mutant-FLT3-positive AML patient samples. Cells were tested in liquid culture (DMEM supplemented with 20% FBS) in the presence of drug. All blood and bone marrow samples from AML patients were obtained under the approval of the Dana-Farber Cancer Institute Institutional Review Board. Primary AML 1: female; 59 years old; <5% bone marrow blasts; 2,600 white blood cell count; hematocrit, 30; 1% peripheral blasts; previous therapy, 3+7 chemotherapy; cytogenetics, normal; mutations, IDH2 (5%), RUNX1 (15%), SRSF2 (16.8%), FLT3-ITD (24 amino acids). Primary AML2: male; 69 years old; 90% bone marrow blasts; 23,000 white blood cell count; hematocrit, 24; 5% peripheral blasts; previous therapy, azacytidine, cytarabline, high-dose Ara-c; cytogenetics, normal; mutations, SRSF2 (54%), ASXL1 (46%), RUNX1 (39.4%), TET2 (insertion) (46%), TET2 (point mutation) (2.8%), TET2 (deletion) (3.5%), FLT3-ITD (51 amino acids).

Polyethylenimine transfection of HEK293T cells. HEK293T cells were cultured in DMEM containing 10% FBS at 37 °C, 5% CO_2 in an incubator and transfected with polyethylenimine (Polysciences) according to the manufacturer's instructions. Ba/F3-FLT3-ITD and MOLM14 cells were maintained in RPMI 1640 medium containing 10% FBS at 37 °C, 5% CO_2 in an incubator.

For the endogenous ubiquitination assay, FLT3-ITD-expressing Ba/F3 cells or MOLM14 cells were treated with HBX19818 or P22077 or with DMSO control for 4 or 24 h at 0, 5, 10 or 20 μM. Cells were collected and then lysed. Immunoprecipitation was carried out with anti-FLT3. Immunoblots were analyzed with anti-ubiquitin or anti-FLT3.

Drug combination studies. For synergy studies, cell viability was initially determined via the trypan blue exclusion assay to quantify cells for cell seeding. Next, the CellTiter-Glo luminescent cell viability assay (Promega, Madison, WI) was used to measure cell growth. Single agents were added simultaneously at fixed ratios to cells. Cell viability was expressed as a function of growth-affected drug-treated versus control cells, and data were analyzed by Calcusyn software (Biosoft, Ferguson, MO, and Cambridge, UK). The Calcusyn program was used for synergy measurement and is based on isobologram generation and the method of Chou and Talalay[37], which uses the median-effect principle to quantify drug-combination effects to determine whether the effects of agents administered together are greater than that expected from a simple addition of their individual effects. After determining the ED_{50} or IC_{50} of each drug, we studied combinations where the concentrations were multiples, or fractions, of the ED_{50}/IC_{50}. Specifically, concentrations of DUB inhibitor and kinase inhibitor were tested alone and in combination as follows: 0.25× IC_{50}, 0.5× IC_{50}, IC_{50}, 2× IC_{50} and 4× IC_{50}. Calcusyn program-generated combination index (CI) values allow for a quantitative measurement of synergism, where synergism is defined by a CI < 1, an additive effect is defined by a CI of 1, and antagonism is defined by a CI > 1. Statistical analysis is automatically part of the computations.

Primagraft study. All animal studies were carried out according to protocols approved by the Dana-Farber Cancer Institute's Institutional Animal Care and Use Committee.

Female NSG mice (6 weeks of age; Jackson Laboratories, Bar Harbor, ME) received either vehicle (10% DMSO + 90% D5W i.p. once per day (QD)) (n = 3) or P22077 (15 mg/kg i.p. QD) (dissolved in 10% DMSO + 90% D5W) (n = 3) for a total of 21 d once the leukemia burden reached the following levels as determined by the percentage of $CD45^+CD33^+$ cells in the peripheral blood: mouse 2E#0 (vehicle), 3.07%; mouse 2E#1 (vehicle), 0.34%; mouse 2E#30 (vehicle), 1.63%; mouse 2D#0, (P22077, 15 mg/kg), 4.68%; mouse 2D#1 (P22077, 15 mg/kg), 1.5%; mouse 2E#10 (P22077, 15 mg/kg), 0.29%. Mice were killed on day 21 of treatment. Bone marrow was flushed from mouse femurs, and spleens and livers were dissected and preserved first in formalin and 24 h later in 70% ethanol.

All AML primagraft samples used in the current study were obtained through the Public Repository of Xenografts (https://www.proxe.org/).

Flow cytometry. Flow cytometry was carried out as previously described, according to standard protocols[24]. Briefly, a Fortessa flow cytometry machine equipped with FACSDiva analytical software was used to analyze the percentage of $FLT3^+$ cells.

doi:10.1038/nchembio.2486

Non-invasive *in vivo* bioluminescence study. All animal studies were performed according to protocols approved by the Dana-Farber Cancer Institute's Institutional Animal Care and Use Committee.

Bioluminescence imaging was performed as described previously[38]. Briefly, for administration to female NCR-nude mice (6–8 weeks of age; Taconic, NY), virus- and mycoplasma-free FLT3-ITD–luc+ Ba/F3 cells were washed and resuspended in 1× PBS and administered via intravenous (i.v.) tail vein injection (0.5×10^6 cells per 250 µL). A sample size of no fewer than eight mice per treatment group was chosen to ensure statistical significance. Anesthetized mice were imaged 2 d after i.v. injection of FLT3-ITD–luc+ Ba/F3 cells to generate a baseline used to establish treatment cohorts with matched tumor burden (mice were randomized and investigators were blinded to group allocation), and total body luminescence was measured as previously described[35]. Drug treatment commenced 2 d after cell injection. Mice were treated with vehicle (10% DMSO in 90% [20%] HPBCD i.p. twice per day (BID)) (n = 8), P22077 (50 mg/kg, 10% DMSO in 90% [20%] HPBCD i.p. BID) (n = 8), P22077 (50 mg/kg, 10% NMP in 90% PEG300) for the times indicated in the relevant figures. Note: one vehicle-treated mouse that showed at least tenfold lower leukemia burden than the other seven vehicle-treated mice in the control group across all time points was removed as an outlier from the final statistical analysis. One P22077 (PO, QD)-treated mouse died prematurely as a result of technical complications unrelated to treatment and consequently was not imaged with the other seven mice from this treatment group.

For *in vivo* assessment of FLT3 protein levels in vehicle-treated and P22077-treated mice, eight female NCR-nude mice (6–8 weeks of age; Taconic, NY) received FLT3-ITD–luc+ Ba/F3 cells via tail vein injection as described above. Mice were imaged and randomized 2 d later to generate a baseline used to establish treatment cohorts with matched tumor burden. At this point, mice were treated with vehicle (10% DMSO in 90% [20%] HPBCD i.p. BID) (n = 4) or P22077 (50 mg/kg, 10% DMSO in 90% [20%] HPBCD i.p. BID) (n = 4) for a total of 4 d. Bone marrow cell suspensions were then analyzed for FLT3 levels by flow cytometry with a PE-conjugated antibody to CD135 (IM2234U; Beckman Coulter, Marseille, France). Flow cytometry was carried out as previously described, according to standard protocols[24]. Briefly, a FACS Fortessa flow cytometry machine equipped with FACSDiva analytical software was used to analyze the percentage of $FLT3^+$ cells.

The statistical significance of differences in bioluminescence between two groups was determined by two-tailed Student's t-test. $P < 0.05$ was considered to indicate statistical significance. The data had similar variance and met the assumptions of the tests.

Labeling with HA-ubiquitin-vinylmethylsulfone. We treated MOLM14 cells for 3 h with P22077 and FLT3-ITD-expressing Ba/F3 cells for 7 h with HBX19818. Cells were harvested, washed with PBS, and lysed in 1% NP-40, 10% glycerol, 2% sodium orthovanadate, and HALT protease inhibitor cocktail (Thermo Fisher). Lysate was diluted to 50 µg in 30 µL of lysis buffer with 1 mM DTT and incubated on ice for 15 min. 0.25 µg of HA-Ub-VS was added, and the sample was gently rocked at room temperature for 30 min, then denatured with LDS sample buffer. 12 µg of lysate was separated by SDS–PAGE, transferred to a nitrocellulose membrane, blocked in milk, and treated with anti-USP10 (D7A5) (rabbit; 8501) (Cell Signaling, Danvers, MA). After washing, the membrane was treated with a 780-nm IRdye goat anti-rabbit IgG (Licor) and imaged with an Odyssey scanner (Licor).

Quantitative real-time polymerase chain reaction. Ba/F3 cells were treated for 23 h, then harvested and washed with PBS. mRNA was extracted with the RNeasy mini kit (Qiagen) and converted to cDNA with SuperScript III reverse transcriptase (Thermo Fisher) and a SimpliAmp thermal cycler (Thermo Fisher). Real-time PCR was carried out in a 96-well plate with TaqMan probes and a 7500 FAST Real-Time PCR system (Thermo Fisher). Relative gene expression was calculated by comparison to a GAPDH reference probe.

Chloroquine rescue. Cells were plated in 24-well plates, and 25 µM chloroquine was added. After 60 min, the appropriate concentration of HBX19818 or P22077 was added. After 3 or 7 h for P22077 or HBX19818, respectively, cells were harvested, washed with 1× PBS, and lysed. 30 µg of lysate was separated by SDS–PAGE, transferred to a nitrocellulose membrane, blocked in milk, and treated with anti-FLT3 (Santa Cruz). After washing, the membrane was treated with a horseradish-peroxidase-conjugated goat anti-rabbit IgG, incubated with Peirce ECL western blotting substrate (Thermo Fisher) and imaged in a dark room.

Protein expression and purification. A construct of human USP10 covering residues 376–798 in the pET28a vector was overexpressed in *Escherichia coli* BL21 (DE3) in TB medium in the presence of 50 mg/ml kanamycin. Cells were grown at 37 °C to an OD of 0.8, cooled to 17 °C, induced with 500 µM isopropyl-1-thio-D-galactopyranoside, incubated overnight at 17 °C, collected by centrifugation, and stored at −80 °C. Cell pellets were sonicated in buffer A (50 mM HEPES, pH 7.5, 300 mM NaCl, 10% glycerol, 10 mM imidazole, and 3 mM BME) and the resulting lysate was centrifuged at 30,000*g* for 30 min. Ni-NTA beads (Qiagen) were mixed with lysate supernatant for 30 min and washed with buffer A. Beads were transferred to an FPLC-compatible column, and the bound protein was washed with 15% buffer B (50 mM HEPES, pH 7.5, 300 mM NaCl, 10% glycerol, 300 mM imidazole, and 3 mM BME) and eluted with 100% buffer B. Thrombin was added to the eluted protein and incubated at 4 °C overnight. The sample was then passed through a HiPrep 26/10 desalting column (GE Healthcare) pre-equilibrated with buffer A without imidazole, and the eluted protein was subjected to a second Ni-NTA step to remove His-tag and thrombin. The eluent was concentrated and passed through a Superdex 200 10/300GL column (GE Healthcare) in a buffer containing 20 mM HEPES, pH 7.5, 150 mM NaCl, and 1 mM DTT. Fractions were pooled, concentrated to 20 mg/ml, and frozen at −80 °C.

Ubiquitin-AMC assay. Recombinant USP10, residues 376–798, was tested for its activity in a ubiquitin-AMC assay in the presence or absence of inhibitors. For this assay, 10 nM USP10 was pre-incubated with different concentrations of inhibitors (or DMSO as a control) in 50 mM HEPES, pH 7.6, 0.5 mM EDTA, 11 µM ovalbumin, 5 mM DTT. The reaction was incubated for 6 h at room temperature before the addition of 2 µM ubiquitin-AMC (Boston Biochem) substrate. We measured the initial rate of the reaction by collecting fluorescence data at 1-min intervals over a 30-min period with a Clariostar fluorescence plate reader at excitation and emission wavelengths of 345 and 445 nm, respectively. The calculated initial rate values were plotted against inhibitor concentrations to determine IC_{50} values.

MALDI-TOF DUB assays. 31 human DUBs were freshly diluted in the reaction buffer (40 mM Tris-HCl, pH 7.6, 5 mM DTT, 0.005% BSA) at different concentrations (**Supplementary Note 1**). Ubiquitin topoisomers (K63, K48, K11 and M1) were diluted to 0.2 µl/µg in dimer buffer (40 mM Tris-HCl, pH 7.6, 0.005% BSA) and used as substrates at a fixed concentration (1.5 µM). The enzymes were pre-incubated with the compounds for 30 min at room temperature at 10 µM final concentration. 0.48 µl of di-ubiquitin topoisomers were added to the reaction mixture to initiate the reaction. The reaction was sealed and incubated for 30 min at room temperature and stopped by the addition of TFA to a final concentration of 2% (vol/vol). 1.050 µl of each reaction was copied in a fresh plate and spiked with 0.15 µl of 16 µM ^{15}N-ubiquitin as an internal standard and mixed 1:1 with freshly prepared 2.5 DHAP matrix (7.6 mg of 2,5-DHAP in 375 ml ethanol and 125 ml of aqueous 12 mg/ml diammonium hydrogen citrate). Reaction and matrix were mixed and 200 nl of mixture was spotted in duplicate onto MTP AnchorChip 1,536 TF (600-mm anchor; Bruker Daltonics).

Mass spectrometry data were acquired on an UltrafleXtreme MALDI-TOF mass spectrometer (Bruker Daltonics) with Compass 1.3 control and processing software. The sample carrier was taught before each analysis to optimize and center laser shooting. Internal calibration was performed before each analysis with the ^{15}N-Ub peak $[M+H]^+$ (average: 8,569.3). Samples were analyzed in automatic mode (AutoXecute, Bruker Daltonics). Ionization was achieved by a 2-kHz smartbeam-II solid state laser with a fixed initial laser power of 60% (laser attenuator offset 68%, range 30%) and detected by the FlashDetector at a detector gain of ×10. Reflector mode was used with optimized voltages for reflector 1 (26.45 kV) and reflector 2 (13.40 kV), ion sources (ion source 1, 25.0 kV; ion source 2, 22.87 kV) and pulsed ion extraction (320 ns). A total

of 3,500 shots were summed up in 'random walk' and with 'large' smartbeam laser focus. Spectra were automatically calibrated on the ^{15}N-Ub *m*/*z* and processed with smoothing (Savitzky–Golay algorithm) and baseline subtraction (TopHat) for reproducible peak annotation on non-resolved isotope distributions: one cycle, 0.2 *m*/*z* for the width. For area calculation, the complete isotopic distribution was taken into account. An in-house-made script was used to report ^{15}N and mono-ubiquitin areas; plotting of graphs, calculation of s.d. and coefficient of variation (%) were processed in Microsoft Excel.

See **Supplementary Note 1** for enzyme dilution and DUB topoisomerase data.

Dynamic BH3 profiling. To determine drug-induced changes in mitochondrial priming, we performed dynamic BH3 profiling as previously described[39,40]. Briefly, 0.4×10^6 cells per well were exposed to drug treatment for 14 h. At the end of the incubation time, cells were washed in PBS, pelleted at 500*g* for 5 min and resuspended in MEB buffer. 15 µl of cell suspension was added to each well of a 384-well plate containing 15 µl of MEB buffer containing 20 µg/mL digitonin and BH3 peptides at twice their final concentration and incubated for 60 min at 26 °C to allow mitochondrial depolarization. Peptide exposure was then terminated by the addition of 10 µl of 4% formaldehyde in PBS for 15 min, followed by neutralization with N2 buffer (1.7 M Tris, 1.25 M glycine, pH 9.1) for 10 min. To determine cytochrome C levels, we diluted anti–cytochrome C (clone 6H2.B4) conjugated to Alexa Fluor 647 (BD Bioscience) 1:50 in 10× staining buffer (10% BSA, 2% Tween-20 and 0.02% sodium azide in PBS) and added 10 µl of this antibody-containing buffer to each well to a final dilution of 1:400. Cells were stained overnight at 4 °C in the dark, and data were acquired on a BD LSR Fortessa analyzer (BD Biosciences). We calculated the priming change (Δ) by comparing the cytochrome C abundance in treated cells to that in DMSO-treated control cells.

Gene knockdown by shRNA. pLKO.1puro lentiviral shRNA vector particles targeting *USP10* and *USP7* were purchased from Sigma-Aldrich (St. Louis, MO). Cells were incubated with the viral particles in the presence of 8 µg/ml Polybrene for 24 h, and the cells were selected with 1–2 µg/ml puromycin for 72 h. After selection, cells were used for the studies described.

For repeat USP10-knockdown studies in MOLM14 cells, viral particles were produced co-transfecting pLKO.1-containing shRNA or scrambled control shRNA (purchased from Sigma-Aldrich) together with psPAX2 (Addgene plasmid #12260) and pMD2.G (Addgene plasmid #12259), concentrated with LENTI-X concentrator (Clontech). MOLM14 cells were then infected in the presence of 5 µg/ml Polybrene, and selection was started 48 h after infection with 1 µg/ml puromycin.

Overexpression of wild-type and mutant USP10 in MOLM14 cells. Flag-HA-USP10 was a gift from the Wade Harper lab (Addgene plasmid #22543)[7]. This construct was used to create the corresponding USP10 catalytic dead construct (USP10C424S) via site-directed mutagenesis according to the manufacturer's instructions. Viral particles were produced co-transfecting wild-type USP10, USP10C424S or control vector together with GAG/POL and VSV-G-containing vectors in HEK293T cells, and concentrated with LENTI-X concentrator (Clontech). MOLM14 cells were then infected in the presence of 5 µg/ml Polybrene, and selection was started 48 h after infection with 1 µg/ml puromycin. Expression of exogenous USP10 was confirmed by HA blot.

Data availability. All data generated during this study are included in this published article (and its supplementary files) or are available from the corresponding author upon request. A **Life Sciences Reporting Summary** for this paper is available.

33. Kelly, L.M. *et al.* FLT3 internal tandem duplication mutations associated with human acute myeloid leukemias induce myeloproliferative disease in a murine bone marrow transplant model. *Blood* **99**, 310–318 (2002).
34. Matsuo, Y. *et al.* Two acute monocytic leukemia (AML-M5a) cell lines (MOLM-13 and MOLM-14) with interclonal phenotypic heterogeneity showing MLL-AF9 fusion resulting from an occult chromosome insertion, ins(11;9)(q23;p22p23). *Leukemia* **11**, 1469–1477 (1997).
35. Armstrong, S.A. *et al.* Inhibition of FLT3 in MLL. Validation of a therapeutic target identified by gene expression based classification. *Cancer Cell* **3**, 173–183 (2003).
36. Weisberg, E. *et al.* Inhibition of mutant FLT3 receptors in leukemia cells by the small molecule tyrosine kinase inhibitor PKC412. *Cancer Cell* **1**, 433–443 (2002).
37. Chou, T.C. & Talalay, P. Quantitative analysis of dose-effect relationships: the combined effects of multiple drugs or enzyme inhibitors. *Adv. Enzyme Regul.* **22**, 27–55 (1984).
38. Weisberg, E. *et al.* Characterization of AMN107, a selective inhibitor of native and mutant Bcr-Abl. *Cancer Cell* **7**, 129–141 (2005).
39. Montero, J. *et al.* Drug-induced death signaling strategy rapidly predicts cancer response to chemotherapy. *Cell* **160**, 977–989 (2015).
40. Pan, R. *et al.* Selective BCL-2 inhibition by ABT-199 causes on-target cell death in acute myeloid leukemia. *Cancer Discov.* **4**, 362–375 (2014).

doi:10.1038/nchembio.2486

Corresponding Author Name: Sara Buhrlage

Manuscript Number: NCHEMB-A161204932A

Reporting Checklist For Life Sciences Articles

This checklist is used to ensure good reporting standards and to improve the reproducibility of published results. For more information, please read Reporting Life Sciences Research. List items are standard for all Nature journal articles but may not apply to all disciplines or manuscripts.

Figure legends

☑ Check here to confirm that the following information is available in all relevant figure legends (or Methods section if too long):

- the **exact sample size (*n*)** for each experimental group/condition, given as a number, not a range;
- a **description of the sample collection** allowing the reader to understand whether the samples represent **technical or biological replicates** (including how many animals, litters, culture, etc.);
- a **statement of how many times the experiment shown was replicated in the laboratory**;
- **definitions of statistical methods and measures**: (For small sample sizes (n<5) descriptive statistics are not appropriate, instead plot individual data points)
  - o very common tests, such as *t*-test, simple χ^2 tests, Wilcoxon and Mann-Whitney tests, can be unambiguously identified by name only, but more complex techniques should be described in the methods section;
  - o are tests one-sided or two-sided?
  - o are there adjustments for multiple comparisons?
  - o **statistical test results**, e.g., ***P* values**;
  - o definition of '**center values**' as **median** or **mean**;
  - o definition of **error bars** as **s.d.** or **s.e.m.** or **c.i.**

This checklist will not be published. Please ensure that the answers to the following questions are reported in the manuscript itself. We encourage you to include a specific subsection in the Methods section for statistics, reagents and animal models. Below, provide the page number or section and paragraph number (e.g. "Page 5" or "Methods, 'reagents' subsection, paragraph 2").

Statistics and general methods	Reported in section/paragraph or page #:
1. How was the sample size chosen to ensure adequate power to detect a pre-specified effect size? (Give section/paragraph or page #)	Methods, Non-invasive bioluminescence study, paragraph 2 (page 21-22)
For animal studies, include a statement about sample size estimate even if no statistical methods were used.	
2. Describe inclusion/exclusion criteria if samples or animals were excluded from the analysis. Were the criteria pre-established? (Give section/paragraph or page #)	Methods, Non-invasive bioluminescence study, paragraph 2 (page 21-22)
3. If a method of randomization was used to determine how samples/animals were allocated to experimental groups and processed, describe it. (Give section/paragraph or page #)	Methods, Non-invasive bioluminescence study, paragraph 2 (page 21-22)
For animal studies, include a statement about randomization even if no randomization was used.	
4. If the investigator was blinded to the group allocation during the experiment and/or when assessing the outcome, state the extent of blinding. (Give section/paragraph or page #)	Methods, Non-invasive bioluminescence study, paragraph 2 (page 21-22)
For animal studies, include a statement about blinding even if no blinding was done.	
5. For every figure, are statistical tests justified as appropriate?	Methods, Non-invasive bioluminescence study, paragraph 4 (page 22)
Do the data meet the assumptions of the tests (e.g., normal distribution)?	hods, Non-invasive bioluminescence study, paragraph 4
Is there an estimate of variation within each group of data?	hods, Non-invasive bioluminescence study, paragraph 4
Is the variance similar between the groups that are being statistically compared? (Give section/paragraph or page #)	hods, Non-invasive bioluminescence study, paragraph 4 (page 22)

(Continues on following page)

Nature Chemical Biology: doi:10.1038/nchembio.2486

Reagents

Reported in section/paragraph or page #:

6. To show that antibodies were profiled for use in the system under study (assay and species), provide a citation, catalog number and/or clone number, supplementary information or reference to an antibody validation profile (e.g., Antibodypedia, 1DegreeBio).

   Methods, Antibodies, paragraph 1-2 (page 18)

7. Cell line identity:

   a. Are any cell lines used in this paper listed in the database of commonly misidentified cell lines maintained by ICLAC (also available in NCBI Biosample)?

   No

   b. If yes, include in the Methods section a scientific justification of their use – indicate here on which page (or section and paragraph) the justification can be found.

   N/A

   c. For each cell line, include in the Methods section a statement that specifies:

   - the source of the cell lines

   Methods, Cell lines and cell culture, paragraph 1 (page 19)

   - have the cell lines been authenticated? If so, by which method?

   Methods, Cell lines and cell culture, paragraph 3 (page 19)

   - have the cell lines been tested for mycoplasma contamination?

   In this checklist, indicate on which page (or section and paragraph) the information can be found.

   Methods, Cell lines and cell culture, paragraph 3 (page 19)

Animal Models

Reported in section/paragraph or page #:

8. Report species, strain, sex and age of animals

   Methods, Primagraft study, paragraph 2 (page 21)
   Methods, Non-invasive bioluminescence study, paragraph 2 (page 21-22)

9. For experiments involving live vertebrates, include a statement of compliance with ethical regulations and identify the committee(s) approving the experiments.

   Methods, Primagraft study, paragraph 2 (page 21)
   Methods, Non-invasive bioluminescence study, paragraph 1 (page 21)

10. We recommend consulting the ARRIVE guidelines (PLoS Biol. 8(6), e1000412,2010) to ensure that other relevant aspects of animal studies are adequately reported.

Human Subjects

Reported in section/paragraph or page #:

11. Identify the committee(s) approving the study protocol.

    N/A

12. Include a statement confirming that informed consent was obtained from all subjects.

    N/A

13. For publication of patient photos, include a statement confirming that consent to publish was obtained.

    N/A

14. Report the clinical trial registration number (at ClinicalTrials.gov or equivalent).

    N/A

15. For phase II and III randomized controlled trials, please refer to the CONSORT statement and submit the CONSORT checklist with your submission.

    N/A

16. For tumor marker prognostic studies, we recommend that you follow the REMARK reporting guidelines.

    N/A

(Continues on following page)

Nature Chemical Biology: doi:10.1038/nchembio.2486

Data Availability

Reported in section/paragraph or page #

17. Please provide a Data Availability statement in the Methods section under "Data Availability". Data availability statements should include, where applicable, accession codes, other unique identifiers and associated web links for publicly available datasets, and any conditions for access of non-publicly available datasets. Where figure source data are provided, statements confirming this should be included in data availability statements. Please refer our data availability and data citations policy for detailed guidance on information that must be provided in this statement.

N/A

Data deposition in a public repository is mandatory for:

a. Protein, DNA and RNA sequences
b. Macromolecular structures
c. Crystallographic data for small molecules
d. Microarray data

Deposition is strongly recommended for many other datasets for which structured public repositories exist; more details on our data policy are available here. We encourage the provision of other source data in supplementary information or in unstructured repositories such as Figshare and Dryad. We encourage publication of Data Descriptors (see Scientific Data) to maximize data reuse

18. If computer code was used to generate results that are central to the paper's conclusions, include a statement in the Methods section under "**Code availability**" to indicate whether and how the code can be accessed. Include version information as necessary and any restrictions on availability.

N/A